frontiers in Earth Science

ORIGINAL RESEARCH
published: 16 July 2021
doi: 10.3389/feart.2021.694906

Modeling of Tectonic-Thermal Evolution of Cretaceous Qingshankou Shale in the Changling Sag, Southern Songliao Basin, NE China

Yuchen Liu[1,2], Bo Liu[2,3]†, LiJuan Cheng[2,3], Jilin Xing[4], Shansi Tian[2,3], Saipeng Huang[2,3] and Suying Dong[1]*

[1]College of Geosciences, Northeast Petroleum University, Daqing, China, [2]Key Laboratory of Continental Shale Hydrocarbon Accumulation and Efficient Development, Ministry of Education, Northeast Petroleum University, Daqing, China, [3]Institute of Unconventional Oil and Gas, Northeast Petroleum University, Daqing, China, [4]PetroChina Jilin Oilfield Company, China National Petroleum Corporation, Songyuan, China

A series of significant shale oil discoveries have been made recently in the Upper Cretaceous Qingshankou Formation in the Songliao Basin, providing a new resource target for shale oil exploration in Northeast China. In this context, an understanding of the tectonic-thermal evolution and maturation history of the Qingshankou Formation is of great significance for shale oil exploration and evaluation. In this study, the thermal history of the Qingshankou Formation since the Late Cretaceous was reconstructed using the paleothermal indicator method. The results indicate that two stages of thermal evolution exist in the southern part of the Songliao Basin: 1) the gradual heating stage during the Late Cretaceous; the heat flow gradually increases during this period and reaches a maximum heat flow value at the end of the Cretaceous. 2) The decline stage since the Neogene; the tectonic activity is relatively stable and the geothermal heat flow is gradually reduced, and the present-day heat flow ranges from 60.1 to 100.7 mW/m^2, with an average of 78.2 mW/m^2. In addition, the maturity history of the organic-rich shale was reconstructed based on the new thermal history. The Cretaceous Qingshankou shales underwent deep burial thermal metamorphism at the end of the Cretaceous, whereas thermal has faded since the Neogene. The hydrocarbon generation and migration since the Late Cretaceous period of K_2qn_1 were modeled based on the maturity model. Two main cooling events took place in the late Nenjiang period and the late Mingshui period in the Changling sag. These two tectonic events controlled the structural style and the formation of shale oil reservoirs in the southern Songliao Basin.

Keywords: tectonic-thermal evolution, basin modeling, shale oil, Qingshankou Formation, southern Songliao Basin

OPEN ACCESS

Edited by:
Guochang Wang,
Saint Francis University, United States

Reviewed by:
Okwudiri Anyiam,
University of Nigeria, Nigeria
Nicolas J. Saintilan,
ETH Zürich, Switzerland

****Correspondence:***
Bo Liu
liubo@nepu.edu.cn

†Present address:
Bo Liu
Northeast Petroleum University,
Daqing, China

Specialty section:
This article was submitted to Economic Geology, a section of the journal Frontiers in Earth Science

Received: *14 April 2021*
Accepted: *21 June 2021*
Published: *16 July 2021*

Citation:
Liu Y, Liu B, Cheng L, Xing J, Tian S, Huang S and Dong S (2021) Modeling of Tectonic-Thermal Evolution of Cretaceous Qingshankou Shale in the Changling Sag, Southern Songliao Basin, NE China. Front. Earth Sci. 9:694906. doi: 10.3389/feart.2021.694906

INTRODUCTION

Rapid growth of the global demand for petroleum and gas resources has promoted exploration and development recently (International Energy Agency, 2011; Wang et al., 2015). Furthermore, with the successful development of shale gas in China, the exploration of shale oil has also been actively promoted (Jia et al., 2018; Sun et al., 2019; Zhang et al., 2020). The resource potential of shale oil in China has been verified and has mainly occurred in continental strata (such as the Cretaceous

formation of the Songliao Basin, the Upper Permian formation of the Junggar Basin and the Santanghu Basin, and the Upper Triassic formation of the Ordos Basin) (Liu et al., 2012; Zou et al., 2013; Gao et al., 2016). Significant exploration breakthroughs and discoveries of shale oil have been made recently in the Upper Cretaceous Qingshankou Formation in the Songliao Basin, providing a new resource target for shale oil exploration in Northeast China (Liu et al., 2017, 2019a, 2019b, 2021; Zhao et al., 2020). Previous studies mainly focused on the geochemical characteristics, lithofacies types, and the shale oil enrichment pattern of the Qingshankou Formation, indicating that the shale oil in the Qingshankou Formation (K_2qn), especially in the first member (K_2qn_1), represents a promising replacement resource for conventional oil (Liu et al., 2017, 2019a, 2019b; Zhang et al., 2020).

Thermal history is of great significance for studying the evolution of formation temperature, hydrocarbon generation, and primary migration histories (Pang et al., 2012; Kosakowski and Krzywiec, 2013; Zuo et al., 2015; Xu et al., 2018; Yu et al., 2020; Nansheng et al., 2021). The current methods for restoring the thermal history of sedimentary basins are generally divided into two categories. One is the paleothermal indicator method, mainly including vitrinite reflectance (Ro), fluid inclusions, clay mineral transformation, fission tracks (AFT and ZFT), and (U-Th)/He (Sweeney and Burnham, 1990; Crowley and Kevin, 1991; Tissot and Welte, 2013). The other uses the thermodynamic model to restore the thermal history of the basin (He et al., 2001, 2011; He, 2014). The former method has higher accuracy for sedimentary basins due to the fact that the simulation results can be verified with measured data. Previous studies mainly focused on the denudation and burial history of the Songliao Basin (Guo et al., 2009; Shi L. et al., 2019). However, little effort was put into reestablishing the thermal history and maturation histories of Qingshankou shale in the southern Songliao Basin. As the main controlling factor for source rock maturity, the pre-Cretaceous thermal history of the southern Songliao Basin should be restored to determine the hydrocarbon generation history and resource potential of the Qingshankou source rocks.

In this study, we reconstructed the tectonic-thermal evolution of the Qingshankou (K_2qn) Formation using a series of vitrinite reflectance. We modeled the thermal evolution of the source rocks in the southern Songliao Basin since the Late Cretaceous. In addition, based on the various geochemical parameters and the simulation method, the timing of hydrocarbon generation and the primary migration of the Qingshankou (K_2qn) source rocks are discussed. This study provides guidelines for shale oil exploration in the Cretaceous Qingshankou Formation of the southern Songliao Basin.

GEOLOGICAL SETTING

The Songliao Basin, located in Northeast China, has a strike extension to the northeast/north-northeast (NE–NNE). It is a composite Mesozoic–Cenozoic sedimentary basin, covering an area of approximately 2.6 $km^2 \times 10^5$ km^2, extending 7.5 m $\times$ 10^4 m in length and (3.3–3.7)×104 m in width. The basin can be subdivided, based on basement morphology, major faults, structural deformation, and sediment distribution, into six first-order tectonic units, including northern plunge, western slope, southwestern uplift, southeastern uplift, northeastern uplift, and central depression (Liu et al., 2021) (**Figure 1A**). With the Songhua River, the Nen River, and the Lalin River as the geographical boundaries, the Songliao Basin can be divided into two parts: the Daqing Oilfield exploration area in the north and the Jilin Oilfield exploration area in the south. The Jilin exploration area in the southern part of the central depression can be further divided into four secondary tectonic units: the Honggang terrace, the Changling sag, the Fuxin uplift belt, and the Huazijing terrace. For this study, the sampling wells are located in the northern part of the Changling sag (**Figure 1B**). The Changling sag is located in the southern part of the central depression. It is a large and gentle depression with a northeast trend and an area of about 6,500 km^2. It connects to the Gulong Sag to the north and is clamped by the Honggang terrace and the Huazijing terrace to the northwest and the southeast, respectively.

The Changling sag exhibits obvious characteristics of fault–depression superimposed sedimentation. During the faulting period, the main sedimentary formations are the Upper Jurassic--Lower Cretaceous Huoshiling Formation (J_3h), Shahezi Formation (K_1sh), Yingcheng Formation (K_1yc), and Denglouku Formation (K_1d), with a maximum thickness of 5,000–7,000 m, which is dominated by terrigenous clastic rocks, volcanic rocks, and pyroclastic rocks. In the depression stage of the basin, the deposited formation includes the Lower Cretaceous Quantou Formation (K_1q) and the Upper Cretaceous Qingshankou Formation (K_2qn), Yaojia Formation (K_2y), Nenjiang Formation (K_2n), Sifangtai Formation (K_2s), and Mingshui Formation (K_2m). These strata are dominated by terrigenous clastic rocks, among which the Qingshankou Formation (K_2qn) serves as the main source rock for the shallower reservoirs in the basin (**Figure 1C**). The Qingshankou Formation can be further divided into the first member (K_2qn_1), the second member (K_2qn_2), and the third member (K_2qn_3). The K_2qn_2 and K_2qn_3 members are widely distributed in the basin with a thickness of 250–550 m. The corresponding lithology is mainly dark gray mudstone and fine sandstone, interbedded. The K_2qn_2 and K_2qn_3 members integrated contact with the K_2qn_1 member and the overlying Yaojia Formation. The lithology of the K_2qn_1 is mainly stable and thick semi-deep lake facies consisting of gray-black mudstone, which was deposited during the first large-scale lacustrine transgression in the basin (Wu et al., 2008; Feng et al., 2010; Liu et al., 2017; Zhang et al., 2020; Liu et al., 2019a, 2019b, 2021). The Songliao Basin has gone through four stages of structural evolution: the volcanic eruption and tension fracture stage (T-J3), the chasmic stage (J_3-K_1), the depression stage (K_1-K_2), and the tectonic reversal phase (K_2-Q).

MODELING PROCEDURE

Burial History Model

Burial history reconstruction is the basis for thermal history modeling. In this part, the basic geological data, including the

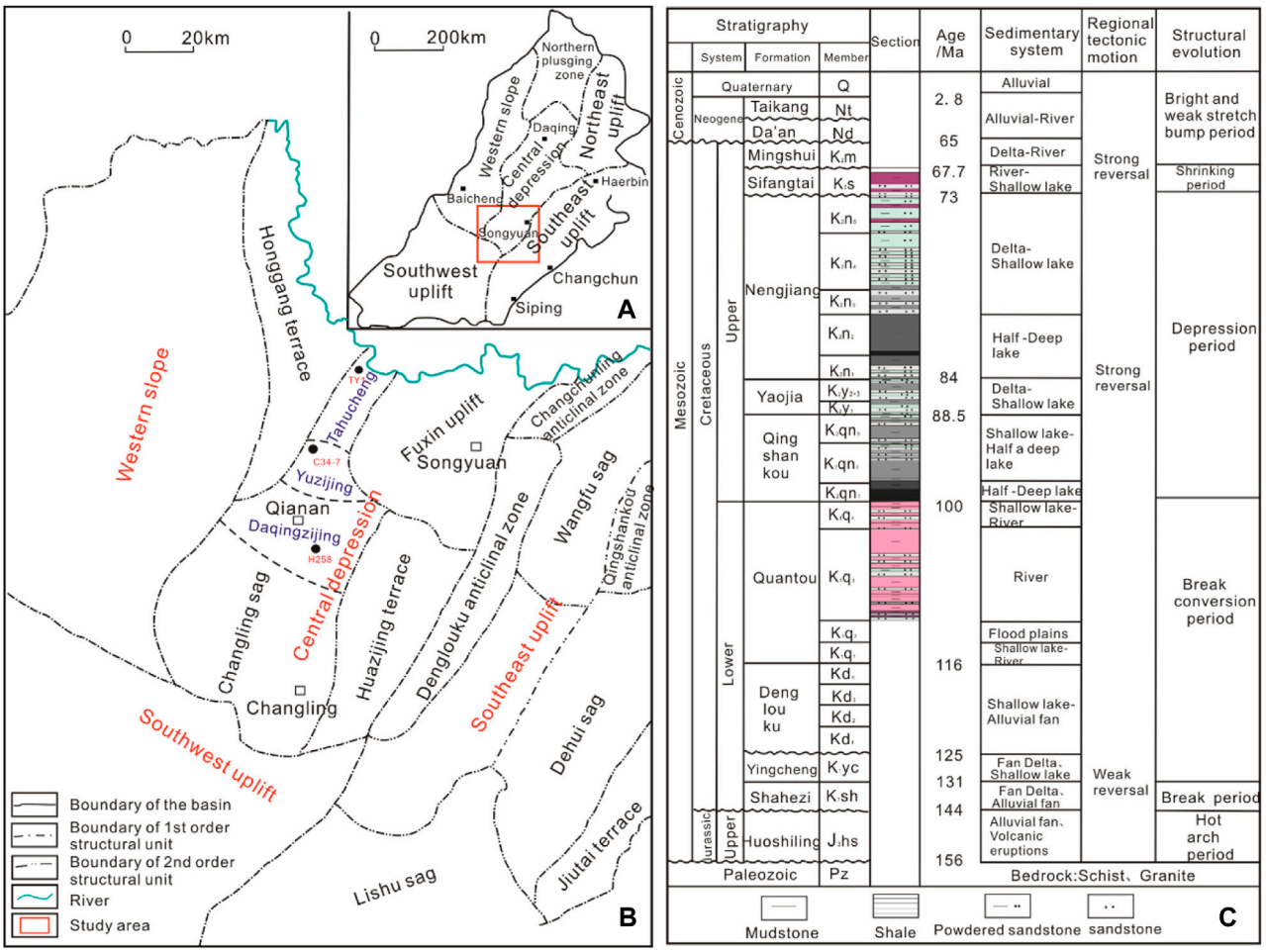

FIGURE 1 | (A) Simplified distribution map of the tectonic units in the Songliao Basin. **(B)** Enlarged view of the southern part of the central depression of the Songliao Basin. **(C)** Composite stratigraphic columnar section of the southern part of the Songliao Basin [modified following Huang et al. (2011)].

thickness, depths, lithologies, and geological ages, referred to the previous studies to construct burial histories (Shi Y. et al., 2019; Guo et al., 2009; Song et al., 2018; Fu et al., 2020). In addition, the erosion events and corresponding eroded thickness are site-specific and were thus considered separately. Since the Late Cretaceous, two main erosion events have taken place in the late Nenjiang Formation and the late Mingshui Formation of the Changling sag. As a result, two corresponding unconformities developed: the unconformity between the Sifangtai and the underlying Nenjiang strata and the unconformity between the Mingshui and the underlying Da'an strata (Guo et al., 2009; Song et al., 2018; Fu et al., 2020). The erosion amounts at the end of the Nenjiang Formation and the Mingshui Formation are 100–300 m and 200–500 m, respectively, and the extent of the erosion amounts gradually decreases from east to west (**Table 1**), which is due to the influence of the Pacific plate subducting westward in the late Paleozoic (Song et al., 2018).

Present Thermal Regime

In the thermal history recovery, the present temperature is one of the important constraints. The well-testing temperature is the ground temperature data obtained during the test oil pressure measurement in the oil-bearing interval of the development well, reflecting the temperature situation of boreholes. The present temperature and the geothermal gradient of forty-three wells in the Qingshankou Formation are shown in **Figure 2** and **Table 2**. The well-testing temperatures of boreholes demonstrated roughly linear temperature–depth relations, which means that the heat transfer in those boreholes is mainly *via* heat conduction. The present temperature in the Daqingzijing area, Yuzijing area, and Tahucheng area of the Qingshankou Formation is 95.7, 102, and 92.2°C, respectively (**Figure 2A**). The current geothermal gradient in the Daqingzijing area, Yuzijing area, and Tahucheng area of the Qingshankou Formation is 36.9, 38.9, and 40.28°C/km, respectively, showing that the present geothermal gradient gradually increases from south to north (**Figure 2B**).

TABLE 1 | Stratigraphy parameters of the Changling sag for burial history modeling.

Well #TY1						Well #C34-7					Well #Hei258				
Formation or event name	Type	Begin age (Ma)	Top depth (m)	Present thickness (m)	Eroded thickness (m)	Formation or event name	Type	Begin age (Ma)	Top depth (m)	Present thickness (m)	Eroded thickness (m)	Formation or event name	Type	Begin age (Ma)	Top depth (m)	Present thickness (m)	Eroded thickness (m)
Q + N	F	0.1	0	75	–	Q + N	F	0.1	0	200	–	Q + N	F	0.1	0	100	–
$E_{2\text{-}3}y$	F	65	75	50	–	$E_{2\text{-}3}y$	F	65	200	25	–	$E_{2\text{-}3}y$	F	65	100	215	–
K_2m-erosion	E	66	–	–	−100	K_2m-erosion	E	66	–	–	−217	K_2m-erosion	E	66	–	–	−100
K_2m	F	67.7	125	300	–	K_2m	F	67.7	225	200	–	K_2m	F	67.7	315	334.5	–
K_2S	F	73	425	318.5	–	K_2S	F	73	425	343	–	K_2S	F	73	649.5	370.5	–
K_2n	F	84	743.5	872.68	–	K_2n-erosion	E	78	–	–	−100	K_2n-erosion	E	78	–	–	−290
K_2y	F	88.5	1,616.18	168.32	–	K_2n	F	84	768	875	–	K_2n	F	84	1,020	653.97	–
K_2qn2-3	F	97	1784.5	502.69	–	K_2y	F	88.5	1,643	140.5	–	K_2y	F	88.5	1,673.97	143.03	–
K_2qn1	F	100	2,287.19	84.41	–	K_2qn2-3	F	97	1783.5	517.51	–	K_2qn2-3	F	97	1817	541.15	–
K_1q	F	116	2,371.6	157.4	–	K_2qn1	F	100	2,301.01	87.42	–	K_2qn1	F	100	2,358.15	105.63	–
						K_1q	F	116	2,388.43	132.57	–	K_1q	F	116	2,463.78	46.22	–

Previous studies have measured the thermal conductivities from 435 core samples in the southern part of the Songliao Basin (Shi L. et al., 2019; Ma et al., 2019). These samples represent almost every lithology in different formations, including sandstone, shale, conglomerate, and volcanic. The frequency distribution histogram of the thermal conductivity of each lithological rock (**Figure 3**) shows that the average thermal conductivity value of shale is the lowest and the distribution range is 1.28–3.79 W/(mK), with a mean of 2.32 ± 0.48 W/(mK). Thus, the thermal conductivity shows a clear increasing trend with increasing depth. The thermal conductivity of sandstone is 1.85–4.48 W/(mK), with an average of 2.67 ± 0.33 W/(mK). The thermal conductivity of the conglomerate is 1.92–3.26 W/(mK), with an average of 2.72 ± 0.33 W/(mK). Finally, the volcanic thermal conductivity is relatively low, with an average of 2.54 ± 0.33W/m/K.

The present-day heat flow directly determines the thermal evolution and is a key input parameter in thermal history evolution (Qiu et al., 2012; Zhu et al., 2018). The surface heat-flow value was calculated using the temperature gradient and the harmonic mean thermal conductivity, as shown in **Eq. 1**. The harmonic mean thermal conductivity of the southern Songliao Basin is about 2.35 ± 0.33 W/(mK), using the measured thermal conductivity values and the thickness of different formations. Present-day heat flows in the southern part of the Songliao Basin range from 60.1 to 100.7 mW/m^2, with an average of 78.2 mW/m^2. Comparison with the northeast uplift, western slope, and southeast uplift of the Songliao Basin reflects a background with typically high heat flow (Ren et al., 2001; Ren et al., 2011), as shown below:

$$q_s = -K_t \cdot \frac{dT}{dZ}, \tag{1}$$

where q_s is the surface heat flow (mW/m^2), K_t is the harmonic mean thermal conductivity [W/(mK)], and $\frac{dT}{dZ}$ is the temperature gradient (°C/m^2).

THERMAL HISTORY RECONSTRUCTION

Analytical Results of Equivalent Vitrinite Reflectance

We measured fifty vitrinite reflectance (%Ro) values from fourteen wells in the southern part of the Songliao Basin (**Table 3**). The vitrinite reflectance values of K_2qn_1 range from 0.99 to 1.36% Ro (average: 1.17% Ro), and the Ro of K_2qn_1 in the Tahucheng area (mean: 1.34%) is higher than that in the Yuzijing and Daqingzijing areas (mean: 1.11 and 1.10%) (**Figure 4**). In this study, the vitrinite reflectance profiles (%Ro) from three typical wells all show increasing trends with depth (**Figure 5**), indicating that all the strata reached a maximum temperature at the same time.

Burial and Thermal Results

This study used the equivalent vitrinite reflectance as the constraint condition and used the ancient heat flow method to recover the thermal history. The main steps are as follows: 1) we need to determine the amount of denudation in each period and

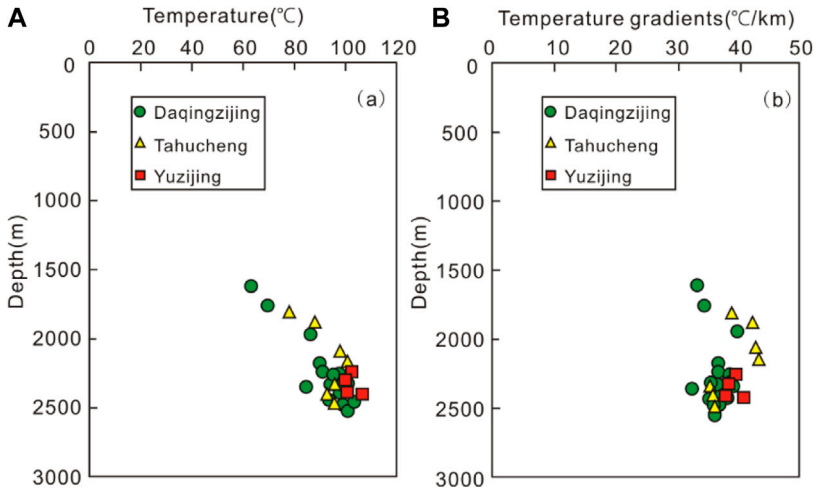

FIGURE 2 | (A) Temperature–depth profiles and **(B)** temperature gradient–depth profiles for the selected boreholes in the southern part of the Songliao Basin.

TABLE 2 | Results of temperature, geothermal gradient, and heat flow in the southern part of the Songliao Basin.

Tectonic unit	Well	Depth (m)	Temperature (°C)	Geothermal gradient (°C/km)	Heat flow (mW/m^2)	Tectonic unit	Well	Depth (m)	Temperature (°C)	Geothermal gradient (°C/km)	Heat flow (mW/m^2)
Daqingzijing area	H103	2,331	92.7	35.8	71.6	Daqingzijing area	H79-29-41	2,423	95.32	35.5	71.0
	H104	2,407	96.67	36.3	72.6		H80	2,521.9	101	36.4	72.7
	H111	2,458.4	102	37.7	75.5		H81	2,362.6	84.6	31.8	63.7
	H113	2,319	98.4	38.5	76.9		H87	2,254.6	96.1	38.5	77.1
	H138-1	2,394	101.15	38.4	76.8		H89-7	1946.6	87.22	40.1	80.2
	H143	2,356.6	99.61	38.4	76.7		H90-1	2,178.2	89.9	37.0	74.0
	H145	2,423.4	98.71	36.9	73.8		H91-1	2,477	101.84	37.4	74.8
	H146	2,442.6	101.7	37.9	75.7		H96-3	2,240.4	91	36.5	73.0
	H163	2,417.72	98.6	37.0	73.9		H98-3	2,306.4	98.6	38.8	77.5
	H47	2,404.6	98.9	37.3	74.6		H197	1760	69.54	34.2	68.4
	H50	2,433.4	100	37.3	74.6		H258	2,457	101.15	37.4	74.8
	H52	2,385.4	93.3	35.2	70.4		H77	2,440	94.31	34.8	69.7
	H57	2,346.2	99.9	38.6	77.3	Tahucheng area	Q160	1,624	63.38	33.3	66.6
	H59	2,512.6	98.9	35.7	71.3		Q180	2,414.9	97.3	36.5	72.9
	H59-11-3	2,508	100.6	36.4	72.8		D15	1894	87.7	41.5	82.9
	H60	2,421	97.3	36.4	72.7		D28	2,170.6	102	42.8	85.6
	H69	2,514	102	36.9	73.8		D45	2,103.6	99	42.7	85.4
	H71	2,304	97.7	38.4	76.8		D56	1812	79.26	38.6	77.3
	H72	2,438.2	101	37.6	75.3		TY1	2,356.6	93.7	35.8	71.6
	H74	2,270	95	37.8	75.6	Yuzijing area	C34-6	2,414.3	105.84	40.0	80.1
	H75	2,352.8	96.7	37.2	74.3		C93	2,383	99.32	37.8	75.6
	H76	2,372.2	98.9	37.8	75.6						

the basic geological parameters such as the thickness of the formation, the depth of the top and the bottom of the formation, lithology, and physical properties; 2) we assume a heat flow evolution history based on the tectonic geological background, and the parallel reaction model (EASY%Ro) is used to calculate the Ro value; 3) repeatedly modify the assumed thermal history so that the measured Ro value and the corresponding EASY% Ro theoretical model calculation value reach the best fit, and it is considered that the thermal history that can correctly reflect the basin's tectonic-thermal evolution process is obtained at this time. The burial and thermal simulation results of three typical wells in different tectonic units of the Changling sag are presented in **Figures 6A,C,E**. The best matches between the measured and the modeled vitrinite reflectance were achieved (**Figures 6B,D,F**), indicating that the simulation results are reliable (Opera et al., 2013; Mohamed et al., 2016). The t-T thermal paths of three typical wells (**Figures 6A,C,E**) show that all samples underwent an overall heating stage after their deposition during the Late Cretaceous, followed by a slow cooling phase from the latest Cretaceous to recent times. In the Cretaceous, affected by the episodic westward compression from the Pacific Plate (Kusky

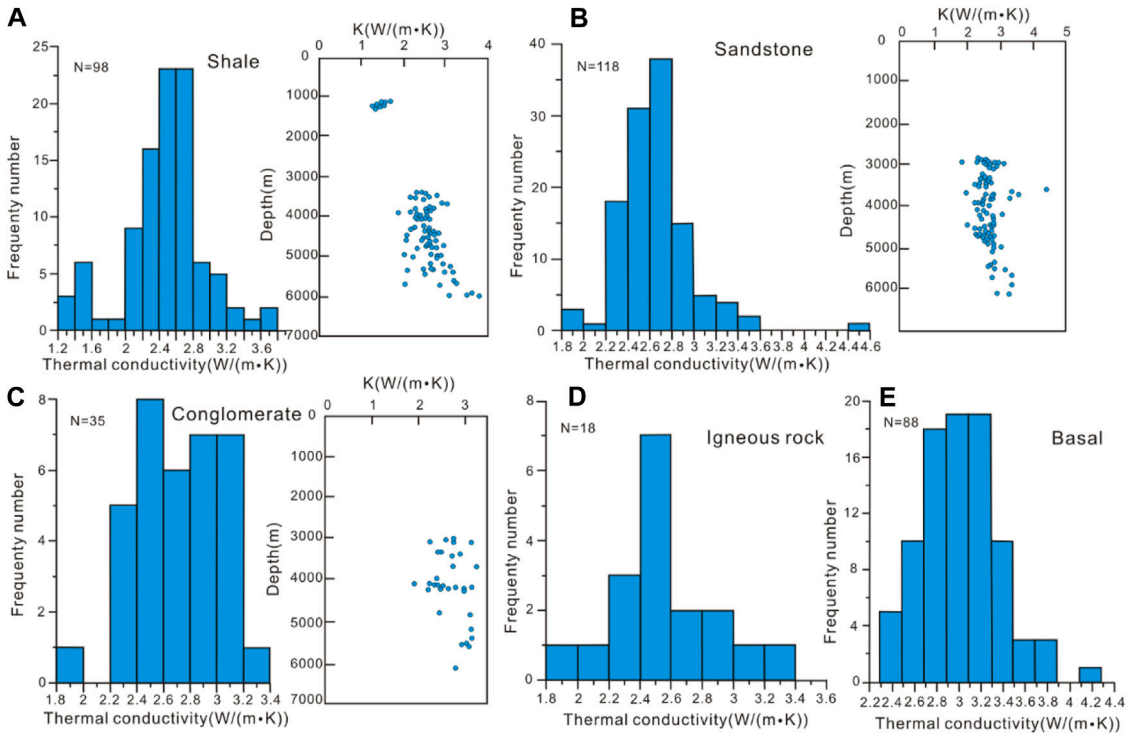

FIGURE 3 | Histogram of measured thermal conductivity of different lithologies in the Songliao Basin. **(A)** Shale; **(B)** sandstone; **(C)** conglomerate; **(D)** igneous rock; and **(E)** basement (modified following Shi Y. et al., 2019).

et al., 2016; Song et al., 2018; Wang et al., 2020), the sedimentary strata of the southern Songliao Basin suffered small-scale erosion. From the Early Cretaceous to the end of the Late Cretaceous, the study area subsided rapidly. The maximum subsidence rate reached nearly 120 m/Ma and reached the maximum burial depth of K_2qn_1 at a depth of ~2,400 m at the end of the Late Cretaceous. In this stage, the geothermal gradient is about ~49°C/km, and the maximum temperature of K_2qn_1 reached ~128°C. Thus, the maximum temperature and heat flow occurred at the end of the Cretaceous (**Figure 7**). This result was also proved by the apatite fission track data published by previous studies (Cheng et al., 2018; Song et al., 2018). There are two phases of heat flow evolution in the southern part of the Songliao Basin: 1) the gradual heating stage during the Late Cretaceous; the heat flow gradually increases during this period and reaches the maximum heat flow value at the end of the Cretaceous. 2) The decline stage since the Neogene; the tectonic activity is relatively stable, and the geothermal heat flow is gradually reduced during this period, while the present-day heat flows range from 60.1 to 100.7 mW/m^2, with an average of 78.2 mW/m^2.

DISCUSSION

Maturation Histories of the Qingshankou Source Rocks

The maturation histories of the source rocks control the timing of hydrocarbon generation and migration (Carminati et al., 2010; Hudson and Hanson, 2010; Pang et al., 2012; Kosakowski and Krzywiec, 2013). The maturity histories of Qingshankou source rocks were calculated based on the constraints of newly obtained Ro data and the current temperature. The thermal model shows that the K_2qn_1 source rocks underwent an overall rapid heating stage after deposition during the Cretaceous and retained thermal maturation until the present day. In the well of C34–7 and H258, the K_2qn_1 source rocks entered the early maturation stage (0.5% < Ro<0.7%) and began to form hydrocarbons since ~85 Ma. At the end of the Late Cretaceous, with the study area subsiding rapidly, the maturity of the source rock entered the middle maturation stage (0.7% < Ro < 1.0%) and formed a large amount of oil. At present, the maturity of the source rock has mostly maintained the characteristics of the end of the Cretaceous. On the other hand, in the well of TY1 of the Tahucheng area, the thermal maturation is slightly higher than that of the Yuzijing and Daqingzijing areas (well C34–7 and H258), and it enters the late maturation stage (1.0% < Ro < 1.3%) at present. It is because the Tahucheng area is the center of deposition, and the buried depth is deeper here than it is in the other two areas. Hence, the thermal maturity of Qingshankou source rocks is slightly higher (**Figure 8**).

Based on the maturity model, the timing of hydrocarbon generation and primary migration since the Late Cretaceous period of K_2qn_1 has been modeled. The results showed that the hydrocarbon generation started from the Late Cretaceous (85 Ma). The maturity of source rocks reached the early oil stage

TABLE 3 | Results of vitrinite reflectance in the southern part of the Songliao Basin.

Well	Depth (m)	Ro (%)	Standard deviation	N	Well	Depth (m)	Ro (%)	Standard deviation	n
TY1	1,615.7	0.71	0.02	16	H258	2,368.4	1.12	0.08	23
TY1	2,370	1.36	0.1	17	H258	2,346	1.1	0.07	23
TY1	2,364.32	1.34	0.07	14	H258	2,464.1	1.18	0.07	30
TY1	2,349.2	1.32	0.07	9	H197	2,516.5	1.04	0.08	29
TY1	2,329.2	1.36	0.06	16	H197	2,529.3	1.09	0.08	30
TY1	2,317	1.21	0.01	10	H197	2,551.5	1.18	0.07	30
TY1	2,286	1.28	0.03	8	H170	1858.2	0.7	0.03	17
TY1	2,335.03	1.3	0.07	15	C34-7	2,342.05	1.1	0.07	15
TY1	2,330.2	1.35	0.06	13	C34-7	2,359.06	1.09	0.06	9
TY1	2,358.5	1.36	0.06	23	C34-7	2,369.5	1.14	0.09	17
H258	1,630	0.62	0.03	14	C19	1,590.1	0.68	0.02	6
H258	2,463.9	1.19	0.08	30	C59	2027.15	0.99	0.05	17
H258	2,451.1	1.17	0.04	30	C59	2030.7	1.07	0.06	30
H258	2,440.1	1.18	0.06	9	C59	2032.7	1.06	0.06	23
H258	2,419.5	1.13	0.08	17	C59	2034.6	1.05	0.06	25
H258	2,399.2	1.17	0.08	30	C59	2036.8	1.03	0.05	26
H258	2,358.03	1.09	0.05	9	H33-2-5	2,433.6	0.82	0.04	20
H258	2,469.7	1.2	0.08	30	H33-2-5	2,417.4	0.78	0.04	16
H258	2,451.1	1.19	0.08	30	H33-2-5	2,445	0.79	0.02	20
H258	2,441	1.16	0.06	23	H48	927.1	0.44	0.03	8
H258	2,436.1	1.18	0.06	23	H41	1,184.7	0.45	0.04	9
H258	2,421.5	1.16	0.08	23	Q193	1,460.5	0.61	0.02	16
H258	2,416.7	1.14	0.07	30	X171	809.6	0.56	0.06	19
H258	2,411.86	1.12	0.06	9	H136	726	0.46	0.04	16
H258	2,401.9	1.18	0.06	30	D51	1,142.9	0.56	0.02	10

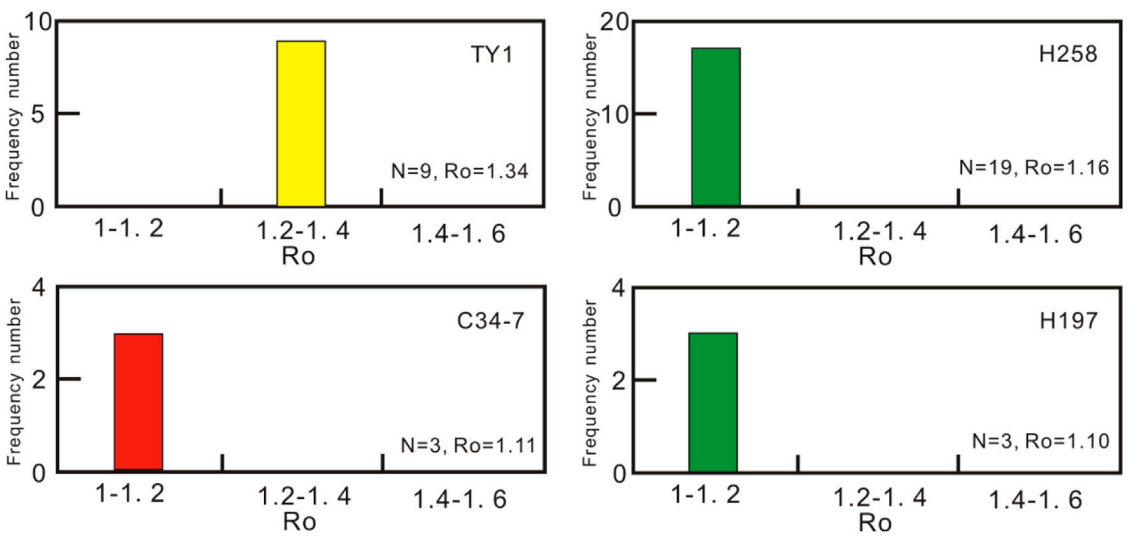

FIGURE 4 | Histograms of vitrinite reflectance of K_2qn_1 in the southern part of the Songliao Basin.

(0.5% < Ro < 0.7%) when a small amount of oil was generated, and the expulsion ratio is almost zero (**Figure 9**). At the end of the Late Cretaceous, the K_2qn_1 source rock began to generate a large amount of hydrocarbon with the rapid increase in the temperature (**Figure 9**), and the hydrocarbon migration took place at the end of the Late Cretaceous (68 Ma). Since the Neogene period, the maturity has mostly maintained characteristics of the end-Cretaceous; the hydrocarbon generation and expulsion of K_2qn_1 increase slowly, and the expulsion ratio reaches about 50%.

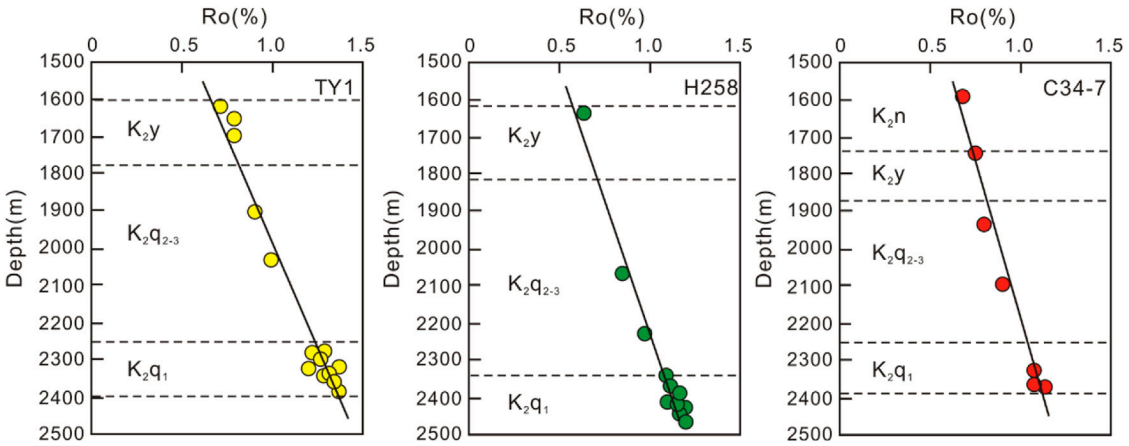

FIGURE 5 | Vitrinite reflectance (%Ro) vs. depth of three typical wells in the southern part of the Songliao Basin.

Additionally, the shale oil expulsion pattern of the K_2qn_1 was established according to the (S1 + S2) and TOC data of the Songliao Basin (Fu and Pang, 2008). The inflection point of the variation of (S1 + S2)/TOC with burial depth is 1,900 m, indicating that the K_2qn_1 began to expel hydrocarbons from 1,900 m. According to the burial and thermal histories, hydrocarbon expulsion started at the end of the Late Cretaceous, consistent with the conclusions of modeling results. With the increase in burial depth, the rate of hydrocarbon expulsion first increases and then decreases, reaching the maximum at about 2,200 m. The corresponding hydrocarbon expulsion rate is about 20.2 mg/g.100 m. At the depth of about 2,400 m, the hydrocarbon expulsion efficiency of the source rock reaches about 50% (**Figure 10**).

In summary, the main hydrocarbon generation stage lasted from the Late Cretaceous to the Paleogene period (68–50 Ma). The rapid burial depth led to an increase in the temperature of the K_2qn_1, which greatly promoted the conversion of organic matter to hydrocarbons. This result led to significant hydrocarbon generation, forming a large amount of oil in the southern part of the Songliao Basin.

Relationship between the thermal history and tectonic evolution.

Since the Late Cretaceous, two main cooling events took place in the late Nenjiang period and the late Mingshui period of the Changling sag. In the late Nenjiang period, the Yanshan movement began to break out, and it was the squeeze fold movement covering the southern part of the Songliao Basin. During this period, the tectonic stress gradually decreases from south to north. So, the extent of cooling in the Daqingzijing area is higher than that in the Tahucheng area. The other squeeze fold movement took place in the late Mingshui period. However, the uplift amplitude is much lower than that of the uplift at the end of the Nenjiang, so the original sedimentary features are retained.

In the late Nenjiang period and the late Mingshui period, there was a period of compression tectonic movement, respectively, and the influence of these two tectonic movements on the formation of shale oil is different. The tectonic movements of the late Nenjiang period mainly controlled the structural style of the Songliao Basin, which was the most intense structural movement affecting the entire Songliao Basin. The structural movement during this period formed the uplift belts in the eastern and southern Songliao Basin. On the other hand, the tectonic movements of the late Mingshui period mainly controlled the formation of shale oil reservoirs. During this period, the source rock matured rapidly, generating and expelling a large amount of oil. Comparing these two movements, the effect of the late Mingshui movement on the formation of shale oil reservoirs in the Changling area is significantly greater than that of the Nenjiang movement.

CONCLUSIONS

The thermal history of the southern Songliao Basin since the Late Cretaceous has been reconstructed using an integrated Ro data and Basinmod situation. The results show that two phases of thermal evolution exist in the southern part of the Songliao Basin: 1) the gradual heating stage from the Late Cretaceous to the Late Cretaceous; the heat flow gradually increases during this period, and it reaches the maximum heat flow value at the end of the Cretaceous. 2) The decline stage since the Neogene; the tectonic activity is relatively stable, and the geothermal heat flow is gradually reduced during this period, while the present-day heat flows range from 60.1 mW/m^2 to 100.7 mW/m^2, with an average of 78.2 mW/m^2.

The maturity histories of the source rocks were modeled based on the new thermal histories. The result indicates that the hydrocarbon generation started from the Late Cretaceous (85 Ma). The maturity of source rocks reached the early oil stage (0.5% < Ro < 0.7%) with a small amount of oil generation, and the expulsion ratio is almost zero. At the end of the Late Cretaceous, with the rapid increase in the temperature of the K_2qn_1 source rock, the source rock began to generate a large amount of hydrocarbon. Meanwhile, the hydrocarbon expulsion occurred at the end of the Late Cretaceous (68 Ma). Since the Neogene period, the maturity

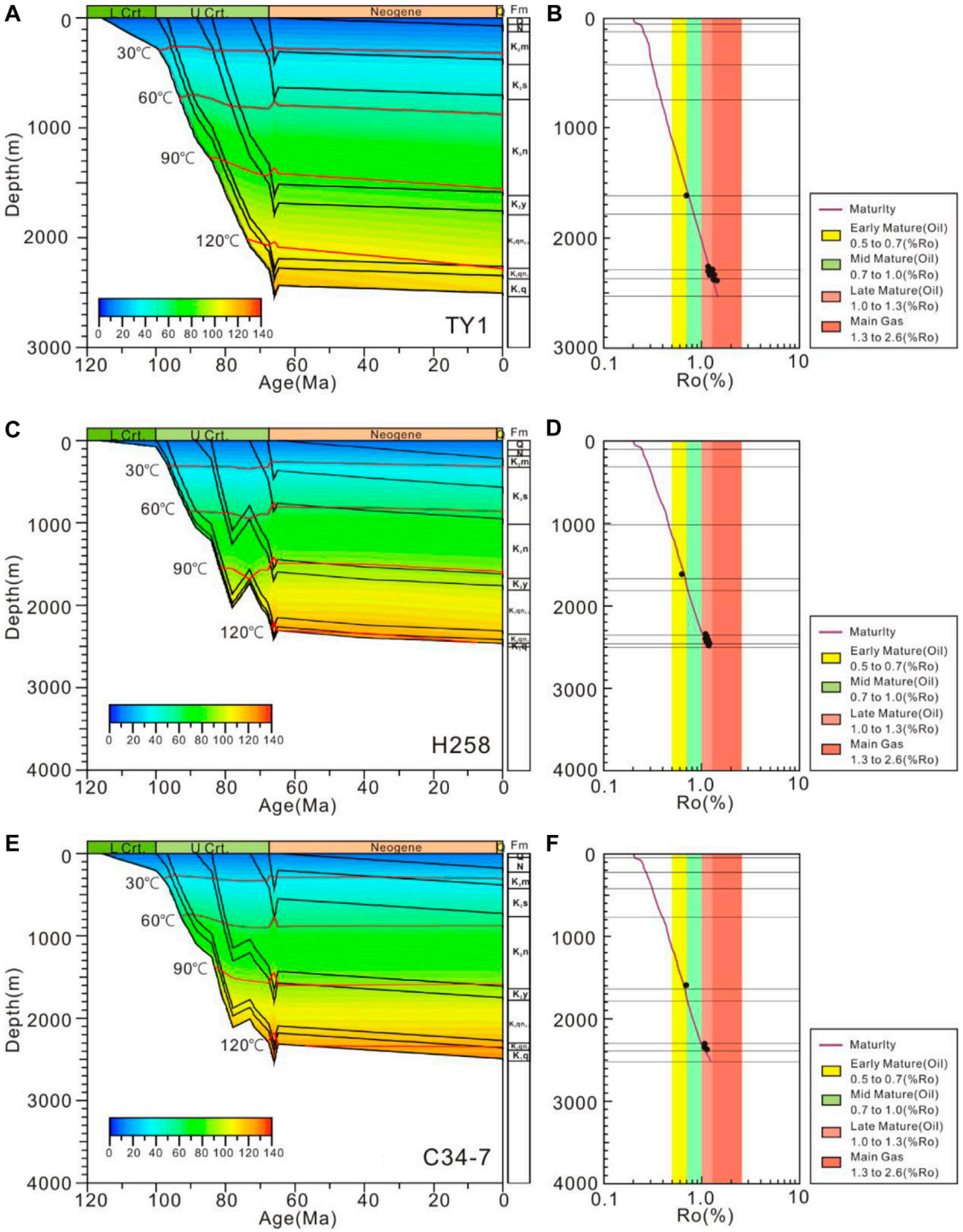

FIGURE 6 | The burial histories of the TY1 well **(A)**, the H258 well **(C)** and the C34-7 well **(E)**, and the thermal models of the TY1 well **(B)**, the H258 well **(D)** and the C34-7 well **(F)** in the southern part of the Songliao Basin.

mostly maintained the characteristics of the end of the Cretaceous; the hydrocarbon generation and expulsion of K_2qn_1 increased slowly, and the expulsion ratio is about 50%.

In summary, the Cretaceous Qingshankou source rocks underwent deep burial thermal metamorphism at the end of the Late Cretaceous and thermal fading since the Neogene. Two main cooling events took place in the late Nenjiang period and the late Mingshui period, which controlled the structural style and the formation of shale oil reservoirs in the southern Songliao Basin.

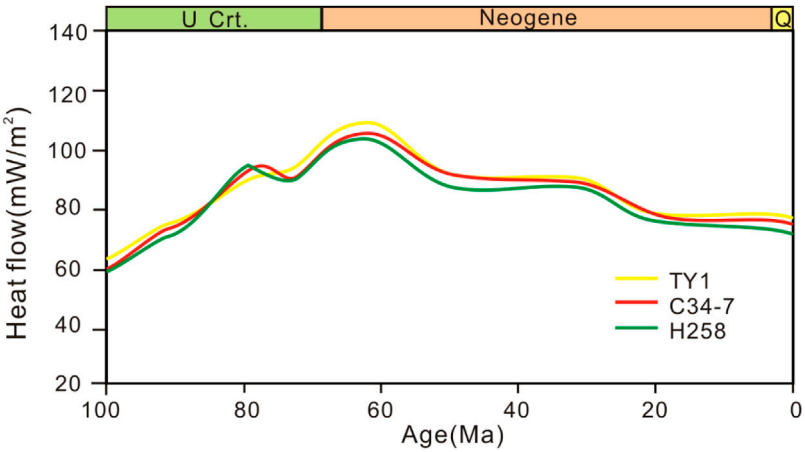

FIGURE 7 | Heat flow history of the typical wells in the southern part of the Songliao Basin.

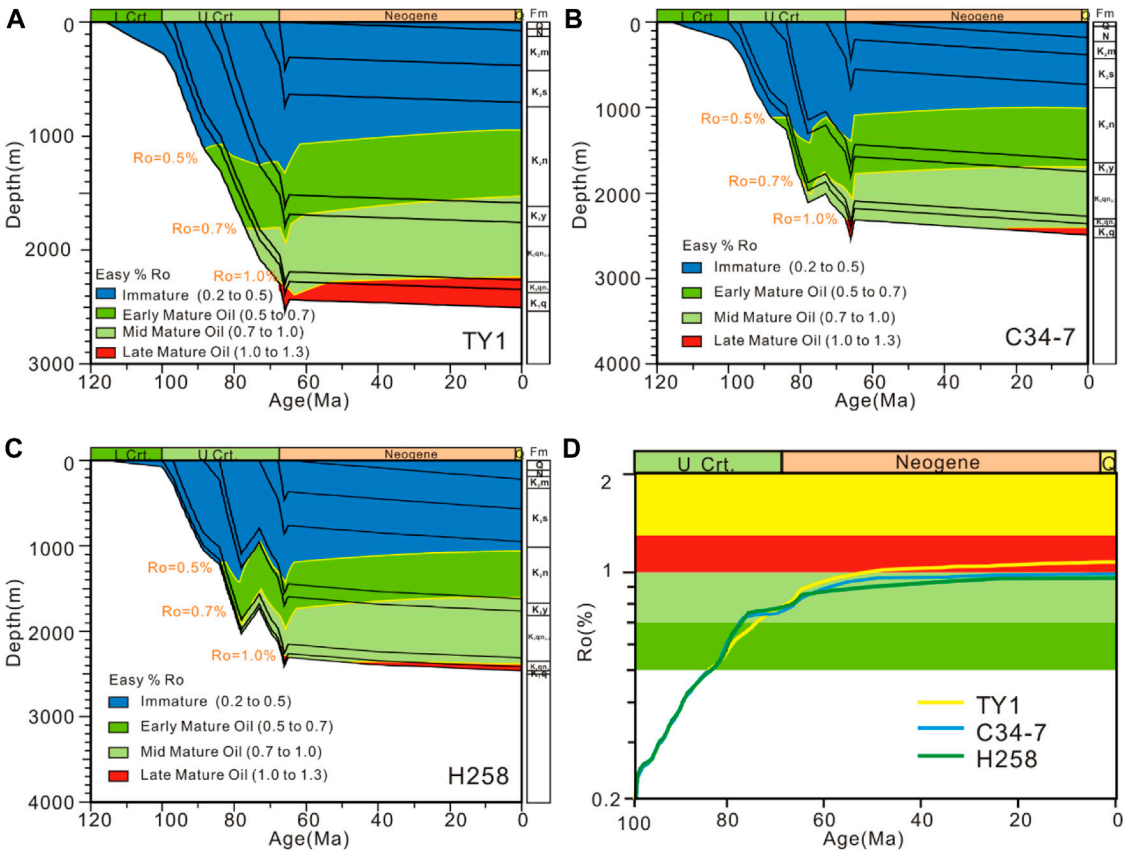

FIGURE 8 | Thermal maturity model of the TY1 well **(A)**, C34-7 well **(B)**, H258 well **(C)**, and the evolution profile of vitrinite reflectance (Ro) of three typical wells **(D)** in the southern part of the Songliao Basin. Timing of hydrocarbon generation and primary migration.

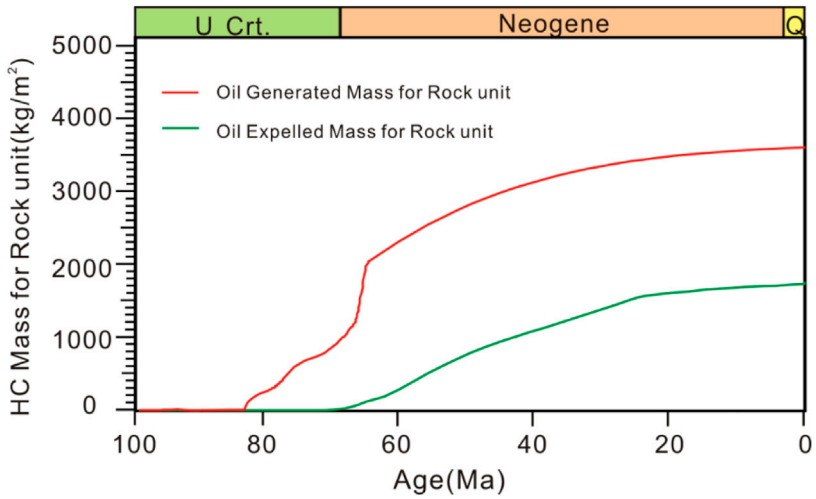

FIGURE 9 | Hydrocarbon generation and primary migration of the K_2qn_1 source rock in the southern part of the Songliao Basin.

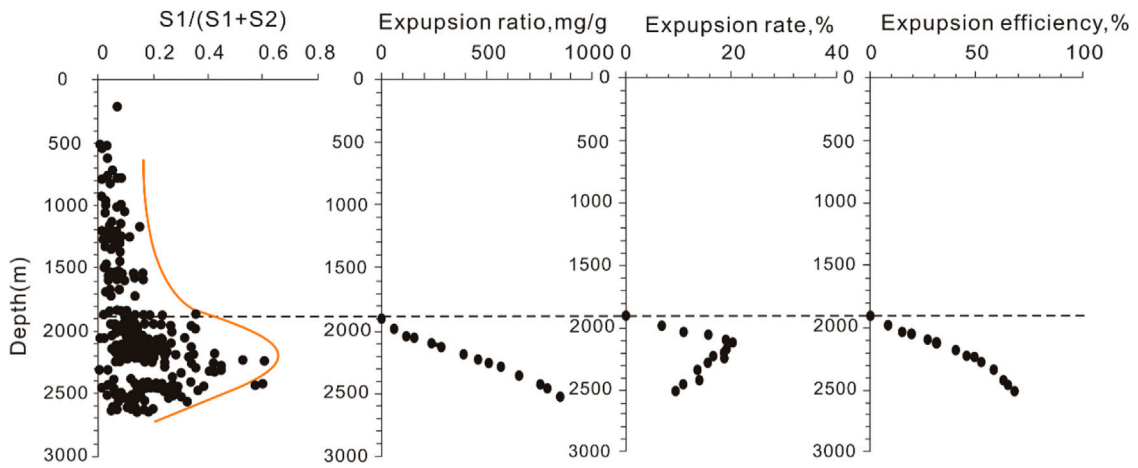

FIGURE 10 | Shale oil expulsion model of the K2qn1 in the southern part of the Songliao Basin [modified following Liu et al. (2017)].

DATA AVAILABILITY STATEMENT

The original contributions presented in the study are included in the article/Supplementary Material, further inquiries can be directed to the corresponding author.

AUTHOR CONTRIBUTIONS

BL devised the project. YL provided the main conceptual ideas and wrote the manuscript. LC, JX, SH, and ST helped with the sampling and data analysis, and SD worked on technical details and part of the thermal analysis. All authors contributed to the article and approved the submitted version.

FUNDING

This work was financially supported by the National Natural Science Foundation of China (42002142 and 41972156) and the Heilongjiang Province Talent Introduction Research Start-up Funds (1305021851).

REFERENCES

Carminati, E., Cavazza, D., Scrocca, D., Fantoni, R., Scotti, P., and Doglioni, C. (2010). Thermal and Tectonic Evolution of the Southern Alps (Northern Italy) Rifting: Coupled Organic Matter Maturity Analysis and Thermokinematic Modeling. *Bulletin* 94, 369–397. doi:10.1306/08240909069

Cheng, Y., Wang, S., Li, Y., Ao, C., Li, Y., Li, J., et al. (2018). Late Cretaceous-Cenozoic Thermochronology in the Southern Songliao Basin, NE China: New Insights from Apatite and Zircon Fission Track Analysis. *J. Asian Earth Sci.* 160, 95–106. doi:10.1016/j.jseaes.2018.04.015

Crowley, K. D., and Kevin, D. (1991). Thermal History of Michigan Basin and Southern Canadian Shield from Apatite Fission Track Analysis. *J. Geophys. Res.* 96 (B1), 697–711. doi:10.1029/90jb02174

Feng, Z., Jia, C., Xie, X., Zhang, S., Feng, Z., and Cross, T. (2010). Tectonostratigraphic Units and Stratigraphic Sequences of the Nonmarine Songliao Basin, Northeast China. *Basin Res.* 22, 79–95. doi:10.1111/j.1365-2117.2009.00445.x

Fu, X., and Pang, X. (2008). Expulsion Characteristics of Qing-1 Member Source Rock, Northern Songliao Basin. *J. Oil Gas Technol.* 30, 166–169.

Fu, X., Shi, H., Meng, Q., Liu, B., Liang, J., and He, J. (2020). Controlling Effects of the Structure and Deposition on the Shale Oil Enrichment: Taking Formation Qn1 in the Central Depression of Songliao Basin as an Instance. *Pet. Geology. Oilfield Develop. Daqing* 39, 56–71.

Gao, J., Liu, G., Yang, W., Zhao, D., Chen, W., and Liu, L. (2016). Geological and Geochemical Characterization of Lacustrine Shale, a Case Study of Lower Jurassic Badaowan Shale in the Junggar Basin, Northwest China. *J. Nat. Gas Sci. Eng.* 31, 15–27. doi:10.1016/j.jngse.2016.03.006

Guo, W., Yu, W., Liu, Z., and Ma, L. (2009). The Burial History of the Southern Songliao Basin. *J. Jilin Univ. (Earth Sci. Edition)* 39, 353–360.

He, L. (2014). Permian to Late Triassic Evolution of the Longmen Shan Foreland Basin (Western Sichuan): Model Results from Both the Lithospheric Extension and Flexure. *J. Asian Earth Sci.* 93, 49–59. doi:10.1016/j.jseaes.2014.07.007

He, L., Wang, K., Xiong, L., and Wang, J. (2001). Heat Flow and thermal History of the South China Sea. *Phys. Earth Planet. Interiors* 126, 211–220. doi:10.1016/s0031-9201(01)00256-4

He, L., Xu, H., and Wang, J. (2011). Thermal Evolution and Dynamic Mechanism of the Sichuan Basin during the Early Permian-Middle Triassic. *Sci. China Earth Sci.* 12, 1884–1891.

Huang, Q. H., Chun, W. H., and Wan, X. Q. (2011). New Progress of Integrated Chronostratigraphy of the Cretaceous in Songliao Basin. *J. Stratigr.* 35, 250–257.

Hudson, S. M., and Hanson, A. D. (2010). Thermal Maturation and Hydrocarbon Migration within La Popa Basin, Northeastern Mexico, with Implications for Other Salt Structures. *Bulletin* 94, 273–291. doi:10.1306/07130907012

International Energy Agency (2011). *World Energy Outlook*. Paris, France: Organization for Economic Cooperation and Development.

Jia, C., Zou, C., Yang, Z., Zhu, R., Chen, Z., Zhang, B., et al. (2018). Significant Progress of continental Petroleum Geological Theory in Basins of Central and Western China. *Pet. Exploration Develop.* 45, 573–588. doi:10.1016/S1876-3804(18)30064-8

Kosakowski, P., Wróbel, M., and Krzywiec, P. (2013). Modelling Hydrocarbon Generation in the Palaeozoic and Mesozoic Successions in Se Poland and West Ukraine. *J. Pet. Geology.* 36, 139–161. doi:10.1111/jpg.12548

Kusky, T. M., Polat, A., Windley, B. F., Burke, K. C., Dewey, J. F., Kidd, W. S. F., et al. (2016). Insights into the Tectonic Evolution of the North China Craton through Comparative Tectonic Analysis: A Record of Outward Growth of Precambrian Continents. *Earth-Science Rev.* 162, 387–432. doi:10.1016/j.earscirev.2016.09.002

Liu, B., Bai, L., Chi, Y., Jia, R., Fu, X., and Yang, L. (2019a). Geochemical Characterization and Quantitative Evaluation of Shale Oil Reservoir by Two-Dimensional Nuclear Magnetic Resonance and Quantitative Grain Fluorescence on Extract: A Case Study from the Qingshankou Formation in Southern Songliao Basin, Northeast China. *Mar. Pet. Geology.* 109, 561–573. doi:10.1016/j.marpetgeo.2019.06.046

Liu, B., He, S., Meng, L., Fu, X., Gong, L., and Wang, H. (2021). Sealing Mechanisms in Volcanic Faulted Reservoirs in Xujiaweizi Extension, Northern Songliao Basin, Northeastern China. *AAPG Bull.* doi:10.1306/03122119048

Liu, B., Lü, Y., Zhao, R., Tu, X., Guo, X., and Shen, Y. (2012). Formation Overpressure and Shale Oil Enrichment in the Shale System of Lucaogou Formation, Malang Sag, Santanghu Basin, NW China. *Pet. Exploration Develop.* 39, 744–750. doi:10.1016/S1876-3804(12)60099-8

Liu, B., Wang, H., Fu, X., Bai, Y., Bai, L., Jia, M., et al. (2019b). Lithofacies and Depositional Setting of a Highly Prospective Lacustrine Shale Oil Succession from the Upper Cretaceous Qingshankou Formation in the Gulong Sag, Northern Songliao Basin, Northeast China. *Bulletin* 103, 405–432. doi:10.1306/08031817416

Liu, C., Wang, Z., Guo, Z., Hong, W., Dun, C., Zhang, X., et al. (2017). Enrichment and Distribution of Shale Oil in the Cretaceous Qingshankou Formation, Songliao Basin, Northeast China. *Mar. Pet. Geology.* 86, 751–770. doi:10.1016/j.marpetgeo.2017.06.034

Ma, F., Wang, G., Sun, Z., Zhang, W., Hou, H., and Guo, X. (2019). An Analysis of Thermal Conductivity in Songliao Basin Based on Logging Parameters. *Acta Geoscientica Sinica* 40, 350–360.

Mohamed, A. Y., Whiteman, A. J., Archer, S. G., and Bowden, S. A. (2016). Thermal Modelling of the Melut basin Sudan and South Sudan: Implications for Hydrocarbon Generation and Migration. *Mar. Pet. Geology.* 77, 746–762. doi:10.1016/j.marpetgeo.2016.07.007

Nansheng, Q., Wen, L., Xiaodong, F., Wenzheng, L., Qiuchen, X., and Chuanqing, Z. (2021). Maturity Evolution of Lower Cambrian Qiongzhusi Formation Shale of the Sichuan Basin. *Mar. Pet. Geology.* 128, 105061. doi:10.1016/j.marpetgeo.2021.105061

Opera, A., Alizadeh, B., Sarafdokht, H., Janbaz, M., Fouladvand, R., and Heidarifard, M. H. (2013). Burial History Reconstruction and thermal Maturity Modeling for the Middle Cretaceous-Early Miocene Petroleum System, Southern Dezful Embayment, SW Iran. *Int. J. Coal Geology.* 120, 1–14. doi:10.1016/j.coal.2013.08.008

Pang, X., Liu, K., Ma, Z., Jiang, Z., Xiang, C., Huo, Z., et al. (2012). Dynamic Field Division of Hydrocarbon Migration, Accumulation and Hydrocarbon Enrichment Rules in Sedimentary Basins. *Acta Geologica Sinica* 86, 1559–1592. doi:10.1111/1755-6724.12023

Qiu, N., Chang, J., Zuo, Y., Wang, J., and Li, H. (2012). Thermal Evolution and Maturation of Lower Paleozoic Source Rocks in the Tarim Basin, Northwest China. *Bulletin* 96, 789–821. doi:10.1306/09071111029

Ren, Z., Xiao, D., Chi, Y., Ren, Y., and Liang, Y. (2011). Restoration of thermal History of the Permo-Carboniferous Basement in the Songliao Basin. *Oil& GAS GEOLOGY.* 32, 430–439.

Ren, Z., Xiao, D., and Chi, Y. (2001). Restoration of Paleotemperature in Songliao Basin. *Pet. Geology. Oilfield Develop. Daqing* 20, 13–16.

Shi, L., Qi, Y., Zhang, Y., Wang, Z., and Wang, B. (2019a). Numerical Simulation of Geohistory of the Qijia Area in the Songliao basin and Geological Significance. *Geology. Exploration* 55 (2), 661–672.

Shi, Y., Jiang, G., Zhang, X., Yuan, Z., Wang, Z., Qiu, Q., et al. (2019b). Present Temperature Field Characterization and Geothermal Resource Assessment in the Harbin Area, Northeast China. *Energy Exploration & Exploitation* 37, 834–848. doi:10.1177/0144598718815922

Song, Y., Ren, J., Liu, K., Shen, C., and Stepashko, A. (2018). Post-rift Anomalous thermal Flux in the Songliao Basin, NE China, as Revealed from Fission Track Thermochronology and Tectonic Analysis. *Palaeogeogr. Palaeoclimatol. Palaeoecol.* 508, 148–165. doi:10.1016/j.palaeo.2018.07.030

Sun, L., Zou, C., Jia, A., Wei, Y., Zhu, R., Wu, S., et al. (2019). Development Characteristics and Orientation of Tight Oil and Gas in China. *Pet. Exploration Develop.* 46, 1073–1087. doi:10.1016/S1876-3804(19)60264-8

Sweeney, J., and Burnham, A. (1990). Evaluation of a Simple Model of Vitrinite Reflectance Based on Chemical Kinetics. *AAPG Bull.* 10, 1559–1570. doi:10.1306/0c9b251f-1710-11d7-8645000102c1865d

Tissot, B., and Welte, D. (2013). *Petroleum Formation and Occurrence*. Springer Science & Business Media.

Wang, J., Feng, L., Steve, M., Tang, X., Gail, T. E., and Mikael, H. (2015). China's Unconventional Oil: A Review of its Resources and Outlook for Long-Term Production. *Energy* 82, 31–42. doi:10.1016/j.energy.2014.12.042

Wang, S., Cheng, Y., Zeng, L., Miao, P., Jin, R., Zhang, T., et al. (2020). Thermal Imprints of Cenozoic Tectonic Evolution in the Songliao Basin, NE China:

Evidence from Apatite Fission-Track (AFT) of CCSD-SK1 Borehole. *J. Asian Earth Sci.* 195, 104353. doi:10.1016/j.jseaes.2020.104353

Wu, H., Zhang, S., and Huang, Q. (2008). Establishment of Floating Astronomical Time Scale for the Terrestrial Late Cretaceous Qingshankou Formation in the Songliao Basin of Northeast China. *Earth Sci. Front.* 15, 159–169. doi:10.1016/s1872-5791(08)60049-4

Xu, Q., Qiu, N., Liu, W., Shen, A., and Wang, X. (2018). Thermal Evolution and Maturation of Sinian and Cambrian Source Rocks in the central Sichuan Basin, Southwest China. *J. Asian Earth Sci.* 164, 143–158. doi:10.1016/j.jseaes.2018.06.015

Yu, K., Ju, Y., and Zhang, B. (2020). Modeling of Tectono-thermal Evolution of Permo-Carboniferous Source Rocks in the Southern Qinshui Basin, China: Consequences for Hydrocarbon Generation. *J. Pet. Sci. Eng.* 193, 107343. doi:10.1016/j.petrol.2020.107343

Zhang, J., Xu, X., Bai, J., Liu, W., Chen, S., Liu, C., et al. (2020). Enrichment and Exploration of Deep Lacustrine Shale Oil in the First Member of Cretaceous Qingshankou Formation, Southern Songliao Basin, NE China. *Pet. Exploration Develop.* 47, 683–698. doi:10.1016/S1876-3804(20)60085-4

Zhao, Z., Littke, R., Zieger, L., Hou, D., and Froidl, F. (2020). Depositional Environment, thermal Maturity and Shale Oil Potential of the Cretaceous Qingshankou Formation in the Eastern Changling Sag, Songliao Basin, China: An Integrated Organic and Inorganic Geochemistry Approach. *Int. J. Coal Geology.* 232, 103621. doi:10.1016/j.coal.2020.103621

Zhu, C., Hu, S., Qiu, N., Jiang, Q., Rao, S., and Liu, S. (2018). Geothermal Constraints on Emeishan Mantle Plume Magmatism: Paleotemperature Reconstruction of the Sichuan Basin, SW China. *Int. J. Earth Sci. (Geol Rundsch)* 107, 71–88. doi:10.1007/s00531-016-1404-2

Zou, C., Yang, Z., Cui, J., Zhu, R., Hou, L., Tao, S., et al. (2013). Formation Mechanism, Geological Characteristics and Development Strategy of Nonmarine Shale Oil in China. *Pet. Exploration Develop.* 40, 15–27. doi:10.1016/S1876-3804(13)60002-6

Zuo, Y.-h., Qiu, N.-s., Hao, Q.-q., Pang, X.-q., Gao, X., Wang, X.-j., et al. (2015). Geothermal Regime and Source Rock thermal Evolution in the Chagan Sag, Inner Mongolia, Northern China. *Mar. Pet. Geology.* 59, 245–267. doi:10.1016/j.marpetgeo.2014.09.001

Conflict of Interest: The author JX was employed by PetroChina Jilin Oilfield Company.

The remaining authors declare that the research was conducted in the absence of any commercial or financial relationships that could be construed as a potential conflict of interest.